Lattice Boltzmann equation linear stability analysis: Thermal and athermal models

D. N. Siebert,* L. A. Hegele, Jr.,† and P. C. Philippi‡
LMPT Mechanical Engineering Department, Federal University of Santa Catarina, 88040-900 Florianopolis, SC, Brazil
(Received 1 October 2007; published 26 February 2008)

Although several thermal lattice Boltzmann models have been proposed, this method has not yet been shown to be able to describe nonisothermal fully compressible flows in a satisfactory manner, mostly due to the presence of important deviations from the advection-diffusion macroscopic equations and also due to numerical instabilities. In this context, this paper presents a linear stability analysis for some lattice Boltzmann models that were recently derived as discrete forms of the continuous Boltzmann equation [P. C. Philippi, L. A. Hegele, Jr., L. O. E. dos Santos, and R. Surmas, Phys. Rev. E **63**, 056702 (2006)], in order to investigate the sources of instability and to find, for each model, the upper and lower limits for the macroscopic variables, between which it is possible to ensure a stable behavior. The results for two-dimensional (2D) lattices with 9, 17, 25, and 37 velocities indicate that increasing the order of approximation of the lattice Boltzmann equation enhances stability. Results are also presented for an athermal 2D nine-velocity model, the accuracy of which has been improved with respect to the standard D2Q9 model, by adding third-order terms in the lattice Boltzmann equation.

DOI: 10.1103/PhysRevE.77.026707 PACS number(s): 47.11.−j, 05.10.−a, 51.10.+y

I. INTRODUCTION

The main goal of the lattice Boltzmann method is to model the dynamical behavior of a fluid on the kinetic level. This purpose is accomplished by calculating the evolution of the distribution function in space and time, given a discrete set of velocities.

The lattice-Boltzmann equation (LBE) was first introduced by McNamara and Zanetti [1], replacing the lattice gas automata Boolean variables, [2], in the discrete collision-propagation equations, with their ensemble averages.

Higuera and Jiménez [3] proposed a linearization of the collision term derived from the Boolean models, recognizing that this full form was unnecessarily complex when the main purpose was to retrieve the hydrodynamic equations.

Following this line of reasoning, Chen *et al.* [4] suggested replacing the collision term with a single relaxation time term, followed by Qian *et al.* [5], who introduced a model based on the Bhatnagar-Gross-Krook (BGK) model [6], retrieving the incompressible Navier-Stokes equations with third-order errors in the local speed.

The BGK collision term describes the relaxation of the distribution function toward an equilibrium distribution. This discrete equilibrium distribution was settled in lattice Boltzmann models by writing it as a second-order polynomial expansion in the local fluid velocity, with adjustable parameters in order to retrieve the mass density, the local velocity and the momentum flux equilibrium moments, which are necessary conditions for satisfying the Navier-Stokes equations.

Thermal lattice Boltzmann models were firstly treated by Alexander *et al.* [7], who extended the Qian *et al.* second-order equilibrium distribution to a third-order model for solving some thermohydrodynamic problems, resulting in a good agreement when compared with analytical solutions.

McNamara and Alder [8], found a set of 13 and 26 restrictions that this expansion must satisfy to retrieve the correct advection-diffusion macroscopic equations, respectively, in two and three dimensions.

Nonlinear deviations in the momentum and energy equations, in the model of Alexander and co-workers, were found by Chen *et al.* [9], who introduced a fourth order polynomial expansion into the equilibrium distribution, fitting adjustable parameters. These authors used combinations of square lattices for satisfying the restrictions imposed by the Chapman-Enskog analysis and found a 16-velocity lattice in two dimensions and a lattice with 41 velocities in three dimensions.

With the exception of McNamara and Zanetti's unconditionally stable LBE, [1], all the above models have stability issues [8,9].

In these studies the equilibrium distribution was written as finite expansions in the local velocity with free parameters that were adjusted to satisfy some main restrictions to retrieve the full advection-diffusion equations. Consequently, there is no formal link connecting the LBE to the Boltzmann equation.

This connection has been first established by He and Luo [10] who directly derived the LBE from the Boltzmann equation for some widely known lattices (D2Q9, D2Q6, D2Q7, D3Q27) by the discretization of the velocity space, using the Gauss-Hermite and Gauss-Radau quadrature. Excluding the above mentioned lattices, the discrete velocity sets obtained by this kind of quadrature do not generate regular space-filling lattices.

Philippi *et al.* [11] derived a construction principle for the LBE considering the velocity discretization problem as a quadrature problem with prescribed abscissas, starting from the Boltzmann equation. It was formally shown that the number of discrete velocities is directly related to the order of approximation of the discrete equilibrium distribution, with respect to the full Maxwell-Boltzmann (MB) distribution and, consequently, to the highest order of the kinetic

*diogo@lmpt.ufsc.br
†hegele@lmpt.ufsc.br
‡philippi@lmpt.ufsc.br

moments that are to be correctly retrieved. Similar results were, almost simultaneously, obtained by Shan *et al.* [12], although using a different procedure.

In this manner, lattices that are able to retrieve second-, third-, and fourth-order terms in the Maxwellian distribution were derived.

The results of Philippi *et al.* were followed by a rigorous Chapman-Enskog analysis of the derived LBE, [13]. It was shown that, when the collision term is written as a BGK single relaxation-time term, the first-order Knudsen internal energy balance equations are only retrieved without errors with the fourth-order LBE.

Three fourth-order two-dimensional models were derived by Philippi *et al.*: The first two based on a set of 25 discrete velocities and the third on a set of 37 velocities. The 37-velocity model was the only one that was written with a complete set of fourth-order Hermite polynomials and since all these three lattice BGK (LBGK) models give the correct thermohydrodynamics, it appeared to be important to determine in which manner the addition of these high-order Hermite polynomials affects the LBE stability in nonisothermal problems.

The stability limits were also obtained in athermal problems, when the temperature deviations are kept null and the sole source of instability is the local speed.

In both the athermal and thermal models it was found that the main reason for instability is the lack of accuracy of the LBE representation with respect to the full continuous Boltzmann equation and that the attainment of larger stability ranges requires an increase in the order of approximation of the LBE.

This is an important result, since this also requires an increase in the number of velocities and is somewhat in contradiction with past studies dealing with simulations using multispeed models where the addition of speeds being led to an increase in instability [14]. In fact, in past studies, the *a posteriore* nature of these methods provided no means to avoid the stability issues in a satisfactory manner.

In this study, it is shown that the construction principle derived by Philippi *et al.* [11], leads to LB models, in which stability can be enhanced by increasing the number of discrete velocities in a systematic way.

It is also shown that stability can be improved by adding higher order Hermite polynomials in the MB polynomial expansion, when the norm of such polynomials is preserved in the discrete space, although this addition has no effect on its first-order Knudsen number behavior. In this paper, this is shown to be true for the D2Q9 athermal LBE.

This paper is organized as follows. In Sec. II the velocity discretization procedure is briefly presented. In Sec. III, some highlights of linear stability analysis are provided. The stability maps obtained for the various models are also presented. Section IV concludes the paper.

II. DISCRETE VELOCITY MODELS FOR THERMAL PROBLEMS

The LBE for collision-propagation schemes can be formally considered as a particular case of an explicit first-order upwind finite-difference numerical approximation of the continuous Boltzmann equation and can be written, for a given point $\boldsymbol{x}$ at a time t, as

$$f_i(\boldsymbol{x}^* + \boldsymbol{c}_i, t^* + 1) - f_i(\boldsymbol{x}^*, t^*) = \Omega_i, \tag{1}$$

where $\boldsymbol{x}^* = \boldsymbol{x}/h$ and $t^* = t/\delta$ are given in dimensionless lattice units, $\boldsymbol{c}_i$ are the usual dimensionless lattice vectors, h and δ are the spatial and time steps and Ω_i is the discretized collision term, usually a collision model such as the BGK single relaxation time model [6] or a multiple relaxation time model [15,16]. In most cases the collision operator Ω_i depends on the explicit form of the local equilibrium distribution function, so when the velocity discretization is performed it is necessary to choose a suitable form for this distribution.

For the BGK collision operator, a Chapman-Enskog analysis shows that the correct hydrodynamic equations are retrieved when the discrete distributions f_i^{eq} have the same moments as the MB distribution up to a third-order term for isothermal problems and some additional fourth-order terms for thermal problems. In many models this function is obtained by a power series of the local velocity $\boldsymbol{u}$, where the coefficients of this expansion are chosen so that f_i^{eq} follows the relation

$$\langle \varphi_p \rangle^{\mathrm{eq}} = \int f^{\mathrm{eq}}(\boldsymbol{\xi}) \varphi_p(\boldsymbol{\xi}) d\boldsymbol{\xi} = \sum_i f_i^{\mathrm{eq}} \varphi_p(\boldsymbol{\xi}_i), \tag{2}$$

where $f^{\mathrm{eq}}(\boldsymbol{\xi})$ is the MB distribution function.

In Philippi *et al.* [11], the discretization of the velocity space is considered as a quadrature problem, i.e., the discrete distributions f_i^{eq} in the right-hand side of Eq. (2) are replaced by the value of a polynomial approximation of the MB distribution evaluated at the pole $\boldsymbol{\xi}_i$, multiplied by a parameter $\mathcal{W}_i$, which represents the weight to be attributed to each velocity vector $\boldsymbol{\xi}_i$ required by the quadrature condition.

Defining a dimensionless velocity $\boldsymbol{\xi}_o = (kT_0/m)^{-1/2}\boldsymbol{\xi}$, the MB distribution can be written as an infinite series of Hermite polynomial tensors $\mathcal{H}^{(n)}_{r_n}(\boldsymbol{\xi}_o)$ [16,17],

$$f^{\mathrm{eq}}(\boldsymbol{\xi}_o) = \left(\frac{m}{kT_0}\right)^{D/2} \frac{e^{-\xi_0^2/2}}{(2\pi)^{D/2}} \sum_n \frac{1}{n!} a^{(n)}_{r_n} \mathcal{H}^{(n)}_{r_n}(\boldsymbol{\xi}_o), \tag{3}$$

where T_0 is a reference and constant temperature, D is the space dimension, and the coefficients $a^{(n)}_{r_n}$ are related to the macroscopic properties at equilibrium and can be found using the orthogonality properties of the Hermite polynomials [13]. An approximated form of the MB distribution $f_i^{\mathrm{eq},N}$ is obtained when the polynomial expansion in Eq. (3) is truncated in the Nth order. It is, nevertheless, important to note that any moment of a velocity polynomial φ_p whose order is equal to or lower than N will be the same as when it is calculated with the full MB distribution:

$$\int f^{\mathrm{eq}} \varphi_p(\boldsymbol{\xi}) d\boldsymbol{\xi} = \int f^{\mathrm{eq},N} \varphi_p(\boldsymbol{\xi}) d\boldsymbol{\xi}. \tag{4}$$

In this manner, to retrieve the correct moments of the MB equilibrium distribution in a discrete velocity space, based on a few velocity vectors, a quadrature is performed, enabling

the integration of the polynomial velocity functions up to a chosen order, without errors. This allows us to write

$$\int f^{\mathrm{eq}}(\boldsymbol{\xi})\varphi_p(\boldsymbol{\xi})d\boldsymbol{\xi} = \sum_i \mathcal{W}_i f^{\mathrm{eq},N}(\boldsymbol{\xi}_i)\varphi_p(\boldsymbol{\xi}_i). \tag{5}$$

The weights $\mathcal{W}_i$ can be written in terms of the conventional dimensionless weights w_i by using

$$\mathcal{W}_i = w_i e^{\xi_o^2/2}\left(\frac{2\pi k T_0}{m}\right)^{D/2}. \tag{6}$$

In Ref. [11], the use of prescribed abcissas was proposed to perform the quadrature, i.e., the velocity vectors $\boldsymbol{\xi}_{o,i}$ are chosen and weights w_i and a scale factor are determined from the quadrature restrictions. This scale factor relates the dimensionless velocity vectors to the usual lattice vectors through $\boldsymbol{\xi}_{o,i}=a\boldsymbol{c}_i$. The authors also showed that when a lattice that is invariant by coordinate permutation and reflection is chosen, the following norm preservation equations assure the orthogonality of the Hermite polynomials in the discrete space:

$$\sum_{i=0}^{b} \omega_i[\mathcal{H}_{r_n}^{(n)}(\boldsymbol{\xi}_{o,i})]^2 = \frac{1}{(2\pi)^{D/2}}\int e^{-\xi_o^2/2}[\mathcal{H}_{r_n}^{(n)}(\boldsymbol{\xi}_o)]^2 d\boldsymbol{\xi}_o \tag{7}$$

for all Hermite polynomial tensors $\mathcal{H}_{r_n}^{(n)}$ with an order lower than or equal to N. In this manner, the discrete velocities are chosen in such a manner as to make the number of variables—the weights and the scale factor—equal to the number of linearly independent equations given by Eq. (7). When this set of equations has a solution, this condition assures that the norm of the Hermite polynomial tensors in discrete space is the same as in continuous space.

By defining $f_i \equiv \mathcal{W}_i f(\boldsymbol{\xi}_i)$, it is possible to obtain the usual form of the discrete equilibrium distribution used in the lattice LBM,

$$f_i^{\mathrm{eq}} = w_i \sum_{n=0}^{N} \frac{1}{n!} a_{r_n}^{(n)} \mathcal{H}_{r_n}^{(n)}(a\boldsymbol{c}_i). \tag{8}$$

Some sets of velocities and the equilibrium distributions for the third- and fourth-order models, which are used in this study, can be found in the Appendix.

III. LINEAR STABILITY ANALYSIS

Instability is a common feature of numeric discrete methods. Since LBM (i) is based on polynomial approximations of the full continuous Boltzmann equation and (ii) discretization is always performed with errors that are proportional to some power of the spatial scale, h, and time step, δ, (iii) and the method is explicit in time, so the LBE is also subject to numerical instabilities.

As discussed in Sec. II, the LBM can be considered as an explicit first-order finite-difference method, so von Neumann linear stability analysis can be applied to the LBE. In the present von Neumann analysis, the aim is to obtain the response of a system, described by a set of equations, which is slightly removed from a given equilibrium state by a small perturbation. When this perturbation is not absorbed by the system itself, such an equilibrium state is considered to be unstable and the mathematical description for this system is unable to describe the system in this state. This is performed using spatial wave perturbations, the effects of which can be superposed, when this physical system is described by linear equations.

Most LBE are nonlinear because they are based on collision operators that are quadratic in f_i. This requires the linearization of the LBE and, although this simplification limits the analysis to small perturbations, it can provide valuable information about the stability behavior of the LBE models. The LBE linearization is performed by developing the collision term in a Taylor series around a global equilibrium distribution $\bar{f}_i$:

$$\bar{f}_i = f_i^{\mathrm{eq}}|_{\bar{\rho},\bar{\boldsymbol{u}},\bar{e}} \tag{9}$$

related to an equilibrium state given by the set of variables $\bar{\rho}$, $\bar{\boldsymbol{u}}$, and $\bar{e}$, where stability is analyzed.

Noting that the collision operator is a function of f_i, i.e., $\Omega_i \equiv \Omega_i(f_0, f_1, \ldots, f_b)$ this Taylor expansion can be written in the form

$$\Omega_i(f) = \Omega_i|_{\bar{f}} + \sum_j \left.\frac{\partial \Omega_i}{\partial \bar{f}_j}\right|_{\bar{f}} \delta f_j + \mathcal{O}(\delta f_j^2), \tag{10}$$

where $\delta f_i \equiv f_i - \bar{f}_i$. The zeroth-order term in Eq. (10) vanishes because $\bar{f}$ is an equilibrium distribution. Replacing this expansion in Eq. (1) and neglecting the second-order terms in δf_i,

$$\delta f_i(\boldsymbol{x}+\boldsymbol{c}_i, t+1) - \delta f_i(\boldsymbol{x}, t) = \sum_{j=0}^{b} \left.\frac{\partial \Omega_i}{\partial \bar{f}_j}\right|_{\bar{f}} (\delta f_j). \tag{11}$$

Performing a discrete Fourier transform in Eq. (11) the following equation for the $\boldsymbol{k}$ wave number component of δf_i is then obtained:

$$\delta f_i(\boldsymbol{k}, t+1) = e^{-i\boldsymbol{c}_i\cdot\boldsymbol{k}} \sum_{j=0}^{b} \left[\delta_{ij} + \left.\frac{\partial \Omega_i}{\partial \bar{f}_j}\right|_{\bar{f}}\right] \delta f_j(\boldsymbol{k}, t). \tag{12}$$

The above equation gives the time evolution of the fluctuation $\delta f_i(\boldsymbol{k}, t)$ from its initial value $\delta f_i(\boldsymbol{k}, 0)$. For convenience this equation will be rewritten using

$$|\delta f_i(\boldsymbol{k}, t+1)\rangle = \hat{L}|\delta f_i(\boldsymbol{k}, t)\rangle, \tag{13}$$

where the Dirac notation for vectors was used and the operator $\hat{L}$ is related to the matrix,

$$L_{ij} = e^{-i\boldsymbol{c}_i\cdot\boldsymbol{k}}\left[\delta_{ij} + \left.\frac{\partial \Omega_i}{\partial \bar{f}_j}\right|_{\bar{f}}\right]. \tag{14}$$

Let the eigenvectors of L_{ij} be denoted by $|z_l\rangle$ and their respective eigenvalues by z_l. In the present case it is suitable to choose these eigenvectors as a basis for representing the perturbed state at $t=0$, $|\delta f(\boldsymbol{k}, 0)\rangle$, because when the $\hat{L}$ operator is applied on these vectors it results in $\hat{L}|z_l\rangle = z_l|z_l\rangle$. In

this manner, after t repeated applications of $\hat{L}$,

$$|\delta f(\boldsymbol{k},t)\rangle = \hat{L}^t|\delta f(\boldsymbol{k},0)\rangle = \sum_{l=0}^{b} b_l(z_l)^t|z_l\rangle, \tag{15}$$

where $b_l=\langle z_l|\,\delta f(\boldsymbol{k},0)\rangle$. Equation (15) shows that the behavior of $|\delta f(\boldsymbol{k},t)\rangle$ can be determined by its eigenvalues z_l and, consequently, that the solution will not diverge for $t\to\infty$ if the complex modulus of the eigenvalues z_l are less than 1 for all values of l.

In conclusion, the investigation of the stability of a physical state given by $\bar{\rho}$, $\bar{u}$ and $\bar{e}$, requires, in von Neumann stability theory, the calculation of the eigenvalues z_l of the L_{ij} matrix. This state is considered to be stable when $|z_l|$ is smaller than 1 for all values of $\boldsymbol{k}$, whose moduli can assume values from 0 to 2π since the L_{ij} matrix elements depend on the wavenumber through the periodic function $e^{-i\boldsymbol{k}\cdot\boldsymbol{c}_i}$.

A. Stability maps of some two-dimensional LBE

In this section the procedure described in the previous section is used to find the stability maps of some two-dimensional LBE proposed by Philippi *et al.*, [11]. We restrict our attention to the BGK, single relaxation time, collision model [6],

$$\Omega_i = \frac{f_i^{\mathrm{eq}} - f_i}{\tau^*}, \tag{16}$$

where $\tau^*=\tau/\delta$ is the dimensionless form of the relaxation time.

The LAPACK++ (Linear Algebra Package for the C++ language) was used to numerically solve the eigenvalue problem, since analytical solutions are only possible for a few particular cases.

The use of numerical methods for obtaining the stability maps is hindered by the large number of diagonalizations required since the matrix must be evaluated for several values of the wave number $\boldsymbol{k}$. In this manner, the dependence of the L_{ij} eigenvalues on the orientation of $\boldsymbol{k}$ was investigated. The results showed that the most unstable case occurs when vectors $\boldsymbol{k}$ and $\boldsymbol{u}$ are parallel, so in the analysis, the orientation of $\boldsymbol{k}$ is restricted to this case. Previous studies on stability have also considered this restriction [18,19].

In particular, Sterling and Chen, [15] have also considered vectors $\boldsymbol{k}$ and $\boldsymbol{u}$ to be parallel to the x axis. Nevertheless, it is shown in Fig. 1 that this assumption can lead to erroneous conclusions. In this figure, the stability limits of the local speed speed $\boldsymbol{u}$ are shown for three different orientations of $\boldsymbol{k}$, for the D2Q9 athermal LBE. The symbol θ gives the angular orientation of vector $\boldsymbol{k}$ with respect to the x axis. In this case, it can be seen that the most critical orientation corresponds to $\theta=\pi/4$ and not to $\theta=0$ as in Sterling and Chen [15]. Thus it can be concluded that the effect of this orientation on the stability limits must be taken into account for each LBE.

For these reasons, for each LBE the stability is investigated considering several values of the wave number k from zero to π distributed in accordance with a fixed interval $\Delta k=0.005$ and several values of the angle θ in the range of 0 to $\pi/4$ spaced by an interval of $\Delta\theta=\pi/100$.

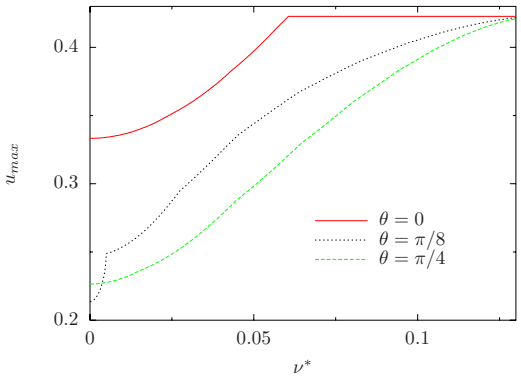

FIG. 1. (Color online) Dependence of the stability limits on the orientation of the wave vector $\boldsymbol{k}$ with respect to the x axis for the D2Q9 LBGK model, where $\nu^*=(\tau^*-1/2)/3$.

1. Athermal models

Our analysis begins with a study of models that use the D2Q9 lattice. The usual D2Q9, first suggested by Qian *et al.* [5], has a second-order equilibrium distribution and can be obtained from the MB distribution by the method described in Sec. II when the order of approximation is set to $N=2$ and the temperature is kept constant and equal to T_o. This lattice was chosen because some third-order moments can be incorporated into this second-order equilibrium distribution using the quadrature procedure described in Sec. II.

In fact, for this LBE, when the weights obtained for the second-order model are used, the norm of the third-order Hermite polynomials $\mathcal{H}^{(3)}_{xxy}$ and $\mathcal{H}^{(3)}_{xyy}$ are also preserved. This allows the inclusion of the related third-order moments in the equilibrium distribution, which takes on the following form:

$$f_i^{\mathrm{eq}} = \rho w_i\left\{1 + 3(\boldsymbol{u}\cdot\boldsymbol{c}_i) + \frac{9}{2}(\boldsymbol{u}\cdot\boldsymbol{c}_i)^2 - \frac{3}{2}u^2 + \frac{27}{2}\left[u_x^2(c_{y,i}u_y)\left(c_{x,i}^2 - \frac{1}{3}\right) + u_y^2(c_{x,i}u_x)\left(c_{y,i}^2 - \frac{1}{3}\right)\right]\right\}. \tag{17}$$

Since this inclusion does not have any effect on the second-order and lower equilibrium moments, the momentum balance macroscopic equations continue to be affected by third-order $\mathcal{O}(u^3)$ errors and the question that remains to be answered is whether the inclusion of these third-order Hermite polynomials has any effect on the LBE stability.

In this manner the D2Q9 stability was analyzed by comparing the D2Q9 LBGK with a second- and a third-order equilibrium distribution. These models were also compared with the Lallemand and Luo, [18], multiple relaxation time (MRT) model, since this model was also built with the aim of improving the LBE stability.

The present analysis can be found in Fig. 2 and is focused on values of the relaxation time very close to its singular limit 1/2. The abscissa was chosen as $1/\tau^*$ in order to compare with previous results from Ref. [18]. It can be observed that both the second- and the third-order LBGK models present a homogeneous decrease in the local speed stability

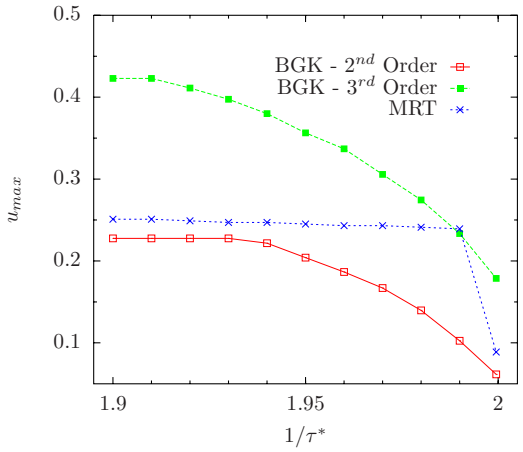

FIG. 2. (Color online) Maximum speed assuring linear stability for models using the D2Q9 lattice.

limit when the relaxation time approaches 1/2, whereas this limit remains insensitive to the τ^* variation in the MRT model, up to $\tau^*=0.50251$. Although the results presented by Lallemand and Luo are not related to quasi-incompressible models, as the present LBGK ones are, they attributed the better performance of the MRT model with respect to the second-order LBGK to the use of high frequency relaxation terms in modeling the collision term.

Figure 2 shows, nevertheless, that the third-order LBGK model has a considerably better performance when compared with the second-order one and with the MRT model in what concerns its stability limits. In this manner, the addition of third-order velocity polynomials largely improve the stability range and this improvement is due to the equilibrium distribution representation itself and not to the use of extra relaxation terms in the collision model. This is an important conclusion, since it avoids the use of MRT dispersion relations for the adjustable parameters—related to the short wavelength nonhydrodynamic moments—to increase numerical stability.

In fact, the improvement of the stability limits by increasing the order of the polynomial approximation to the full MB equilibrium distribution in LBGK models has shown to be a general result. This can be seen in Fig. 3, where the second order LBGK D2Q9 model is compared with the full third-order D2V17 and with the full fourth-order D2V37 models, derived by Philippi *et al.* [11]. These LBE are shown in the Appendix of the present paper. For the athermal results shown in Fig. 3 the temperature T was kept constant, $T=T_0$.

In the use of LBM it is of great interest to solve high Reynolds number flow problems and this usually requires dealing with low values of the kinematic viscosity and, consequently, with relaxation times very close to their lower limits. A Chanpman-Enskog analysis, [13], shows that for these three models the dimensionless kinematic viscosity is given by

$$\nu^* = \frac{1}{a^2}\left(\tau^* - \frac{1}{2}\right). \tag{18}$$

Since the scale factor a is dependent on the lattice, it is better to draw the lattice maps in terms of the dimensionless kine-

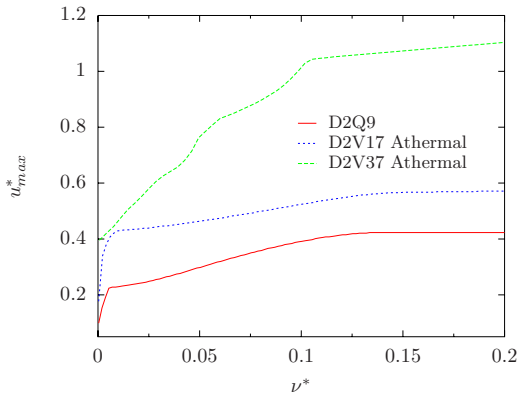

FIG. 3. (Color online) Stability map for the second-, third-, and fourth-order athermal models.

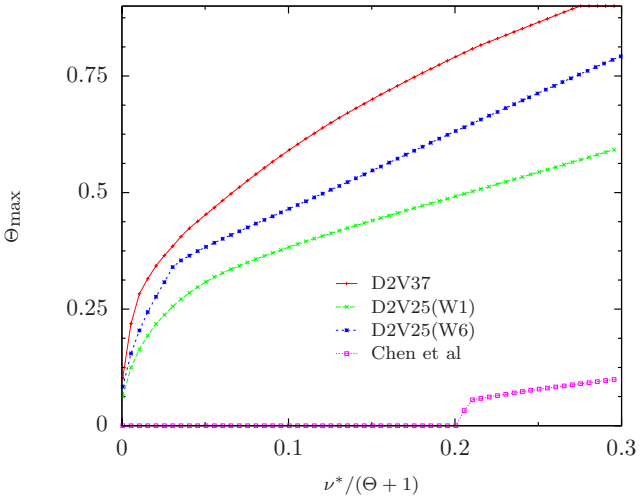

(a) $\Theta > 0$

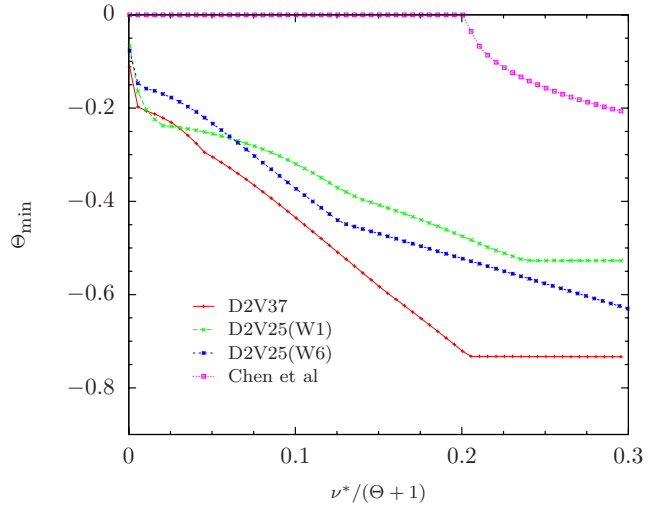

(b) $\Theta < 0$

FIG. 4. (Color online) Positive and negative maximum stable values for deviation of the temperature from T_o for $u^*=0$.

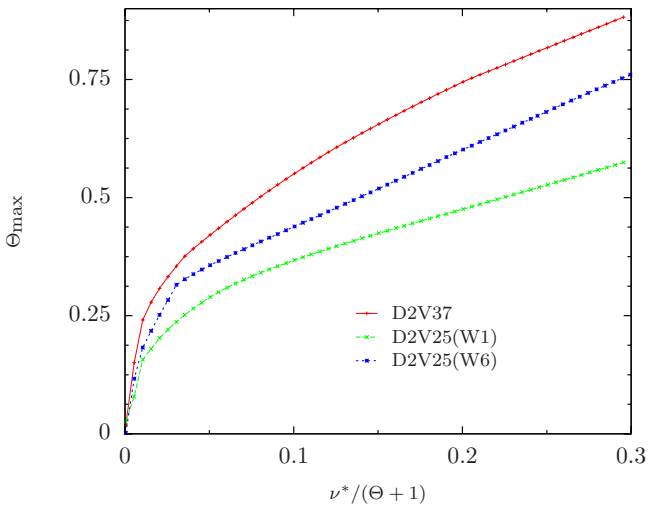

(a) $\Theta > 0$

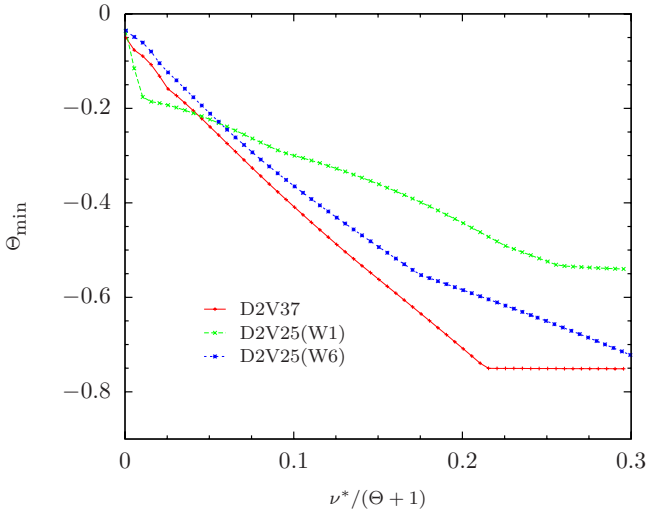

(b) $\Theta < 0$

FIG. 5. (Color online) Positive and negative maximum stable values for deviation of the temperature from T_o for $u^*=0.2$.

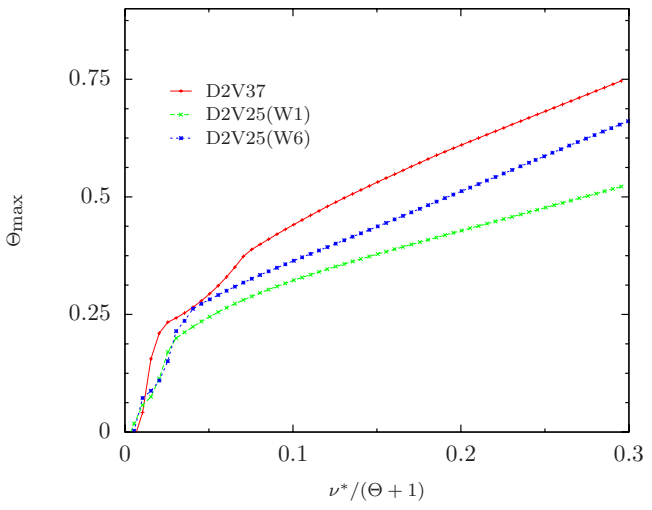

(a) $\Theta > 0$

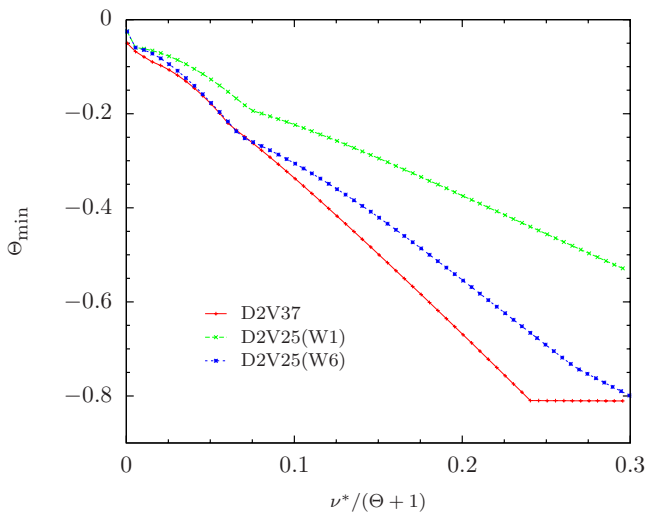

(b) $\Theta < 0$

FIG. 6. (Color online) Positive and negative maximum stable values for deviation of the temperature from T_o for $u^*=0.4$.

matic viscosity, instead of using the dimensionless relaxation time τ^* since in a great number of physical problems the parameter of interest is the Reynolds number.

Figure 3 shows a detailed stability map for the local velocity for these three models. It can be observed that the stability limits remain larger for higher order LB models even for very small viscosity values. In the case of the D2V37 athermal model, the maximum velocity predicted, in this analysis was $u^*=0.4$, corresponding to a dimensionless kinematic viscosity of $\nu^*=0.0007$.

2. Thermal models

The main purpose of this study is to understand the reasons why the LBE becomes unstable when the temperature deviations increase. To address this subject, the temperature deviations are expressed by

$$\Theta = \frac{T}{T_o} - 1. \tag{19}$$

The thermal LBE, D2V25(W1), D2V25(W2), and D2V37 presented by Philippi *et al.* [11], are investigated and compared with the thermal model of Chen *et al.* [9], since the latter model retrieves the correct macroscopic balance equations for the momentum and energy.

For the models considered in this analysis the dimensionless kinematic viscosity can be written as

$$\nu^* = \frac{(\Theta+1)}{a^2}\left(\tau^* - \frac{1}{2}\right) \tag{20}$$

and the Prandtl number is equal to 1.

Since the viscosity is dependent on the temperature the stability maps were drawn in terms of $\nu^*/(\Theta+1)$. Consider-

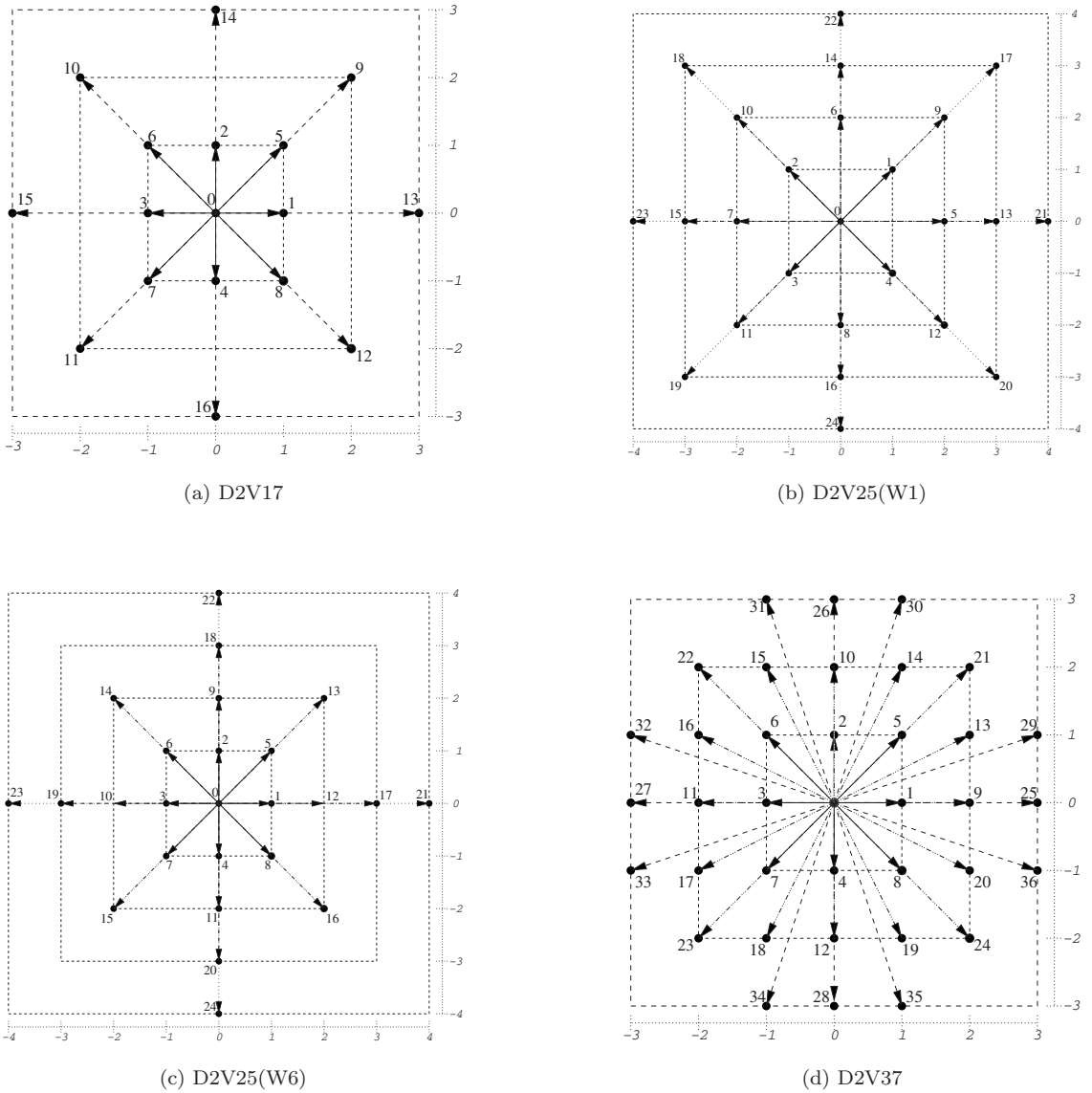

(a) D2V17

(b) D2V25(W1)

(c) D2V25(W6)

(d) D2V37

FIG. 7. Lattice vectors $\boldsymbol{c}_i$ for third and fourth order models.

ing that the model of Chen *et al.* has, in principle, no scale factor, the value of a for this model was set in such way that the macroscopic state with $\Theta=0$ is the most stable one.

Figure 4 shows both the (a) positive and (b) negative limits for Θ, considering a null local velocity. It can be observed that the model of Chen *et al.* gives no stable values for the temperature deviations, when $\nu^*/(\Theta+1)<0.2$. The results also show that the models proposed by Philippi *et al.* are stable over a large interval of temperatures even when the kinematic viscosity attains very low values. As in the previous section, the higher order D2V37 model has a broad stability range, followed by the D2V25(W6) LBE, although the D2V25(W1) LBE may appear to be more stable for low viscosity values, $\nu^*/(\Theta+1)<0.02$. It can also be noted that the curves are not symmetric with respect to the axis $\Theta=0$. This was to be expected since Θ is related to the internal energy through $e^*=(\Theta+1)/a^2$.

Figures 5 and 6 give the same Θ stability maps when the local velocity u^* increases, attaining the values $u^*=0.2$ and $u^*=0.4$. The Chen *et al.* model is not included since this model does not have any stability window in these stability maps when the local velocity $u^*\geq 0.2$.

As expected, an increase in the local velocity reduces the range of temperature deviations which results in a stable behavior.

The thermal LB models derived by Philippi *et al.* [11], are still stable over a large range of temperature deviations. Although this range decreases with u^* and disappears for very small values of $\nu^*/(\Theta+1)$ these results show that the D2V25 and D2V37 have very improved stability ranges when compared to past models.

Another important conclusion from this and the previous sections is that the main reason for LBE instability is a poor discrete representation of the continuous Boltzmann equation. In fact, although the present analysis is restricted to LBGK equations, in all the stability maps given in Figs. 4–6, stability is always increased when the LBE is derived in a systematic way from the continuous Boltzmann equation,

leading to enhanced higher-order representations of the continuous Boltzmann equation.

IV. CONCLUSION

The main purpose of this paper was to investigate the extent to which a temperature deviation can be supported by a thermal LBE, particularly when its order of approximation to the Boltzmann equation is increased. In this way, a linear stability analysis of several thermal and athermal models was performed.

Contrary to some conclusions that have been reported in LBE literature [14,18,20], our results show that the use of additional speeds improves the stability, when the LBE is derived in a systematic way, considering it as a polynomial approximation to the continuous Boltzmann equation. Also the quadrature weights and scaling factor must be chosen in such a way as to preserve the same moments as the MB distribution.

It has also been shown that for athermal models, the use of a higher order LBE increases the linear stability limits of the local velocity, $\boldsymbol{u}$. In particular, the use of more complete equilibrium distributions by the addition of suitable higher order Hermite polynomials gives a better stability to the LBE, although this does not affect the macroscopic behavior of its Knudsen first-order moments.

The large number of discrete velocities, which makes the present thermal LBE difficult to handle in computers in practical advection-diffusion problems, is a direct consequence of the adoption of a discrete collision-propagation scheme in deriving these models. The number of discrete velocities can be suitably reduced by using alternative finite-difference time and spatial discretization of the stream term in the Boltzmann equation and is the subject of a ongoing work being carried out by the authors.

In the same manner, although the present analysis was restricted to LBGK models, it can be easily extended to collision models that are beyond the BGK framework. An LBE with two relaxation times LBE that avoids the unitary Prandtl number restriction was systematically derived by the authors, [16], and will be the subject of a future paper on stability analysis.

ACKNOWLEDGMENTS

The authors are greatly indebted to CAPES (Coordenacao de Aperfeioamento de Pessoal de Nivel Superior), CNPq (Conselho Nacional de Desenvolvimento Cientifico e Tecnologico), Finep (Financiadora de Estudos e Projetos), and Petrobras (Petroleo Brasileiro SA).

APPENDIX: TWO-DIMENSIONAL LATTICES

The procedure described in Sec. II can be used to obtain the LBE as progressively enhanced representations of the continuous Boltzmann equation with the BGK collision model, when the order of the polynomial approximation to the MB equilibrium distribution is increased.

Seventeen discrete velocities were required for a full third-order model, resulting in the D2V17 LBE shown in Fig. 7(a) whose equilibrium distribution is given by

$$f_i^{\mathrm{eq},3} = \rho w_i \left[1 - \Theta + a^2 \boldsymbol{c}_i \cdot \boldsymbol{u} + \frac{a^4}{2}(\boldsymbol{c}_i \cdot \boldsymbol{u})^2 - \frac{a^2 u^2}{2} + \frac{a^2 c_i^2 \Theta}{2} + \frac{a^4 \Theta}{2} c_i^2 (\boldsymbol{c}_i \cdot \boldsymbol{u}) + \frac{a^6}{6}(\boldsymbol{c}_i \cdot \boldsymbol{u})^3 - 2\Theta a^2 (\boldsymbol{c}_i \cdot \boldsymbol{u}) - \frac{a^4 u^2}{2} \boldsymbol{c}_i \cdot \boldsymbol{u} \right], \tag{A1}$$

where the weights and the scaling factor a are shown in Table I.

TABLE I. Weights and scaling factor of D2V17 model.

i	w_i
0	$\frac{575+193\sqrt{193}}{8100}$
1–4	$\frac{3355-91\sqrt{193}}{18000}$
5–8	$\frac{655+17\sqrt{193}}{27000}$
9–12	$\frac{685-49\sqrt{193}}{54000}$
13–16	$\frac{1445-101\sqrt{193}}{162000}$
a	$\sqrt{\frac{5(25+\sqrt{193})}{72}}$

The models with fourth-order terms in the equilibrium distribution are the D2V25(W1), D2V25(W6), and the D2V37.

TABLE II. Weights and scaling factor of the D2V25 models.

i	D2V25(W1)	D2V25(W6)
0	$\frac{2592a^8-7380a^6+11165a^4-7950a^2+2148}{2592a^8}$	$\frac{16(6849-1135\sqrt{33})}{3(15-\sqrt{33})^4}$
1–4	$\frac{12a^4-13a^2+4}{32a^8}$	$\frac{64(2619-437\sqrt{33})}{15(15-\sqrt{33})^4}$
5–8	$\frac{-24a^6-89a^4-80a^2+24}{240a^8}$	$\frac{512(7-\sqrt{33})}{(15-\sqrt{33})^4}$
9–12	$\frac{-3a^4+10a^2-4}{320a^8}$	$\frac{8(159+47\sqrt{33})}{15(15-\sqrt{33})^4}$
13–16	$\frac{144a^6-574a^4+735a^2-264}{11340a^8}$	$\frac{2(17+\sqrt{33})}{(15-\sqrt{33})^4}$
17–20	$\frac{4a^4-15a^2+12}{12960a^8}$	$\frac{64(99-13\sqrt{33})}{105(15-\sqrt{33})^4}$
21–24	$\frac{-12a^6+49a^4-70a^2+36}{13440a^8}$	$\frac{4(-93+19\sqrt{33})}{105(15-\sqrt{33})^4}$
a	$\frac{1}{6}\sqrt{\frac{1}{2}\left(\frac{53(1081-18\sqrt{52413})^{1/3}+251-(1081-18\sqrt{52413})^{2/3}}{(1081-18\sqrt{52413})^{1/3}}\right)}$	$\frac{1}{2}\sqrt{\frac{1}{2}(15-\sqrt{33})}$

The 25-velocity lattices are shown in Figs. 7(b) and 7(c). These two LBE recover the complete Knudsen first-order advection-diffusion equations, without errors and their equilibrium distribution can be written as

$$f_i^{\mathrm{eq},4i} = f_i^{\mathrm{eq},3} + \rho w_i \left[\frac{a^4}{8}\Theta^2 c_i^4 - a^2\Theta^2 c_i^2 + a^2\Theta u^2 - \frac{a^4}{4}u^2 c_i^2\Theta - \frac{3a^4}{2}\Theta(\boldsymbol{u}\cdot\boldsymbol{c}_i)^2 + \frac{a^6}{4}\Theta(\boldsymbol{u}\cdot\boldsymbol{c}_i)^2 c_i^2 + \frac{a^4}{8}u^4 - \frac{a^6}{4}(\boldsymbol{u}\cdot\boldsymbol{c}_i)^2 u^2 - \frac{a^8}{192}u^4 c_i^2 + \frac{a^8}{24}u^2 c_i^2(\boldsymbol{u}\cdot\boldsymbol{c}_i)^2 \right]. \quad \text{(A2)}$$

The weights and the scaling factor for these models can be found in Table II.

Full fourth-order models required a set of 37 lattice vectors in two-dimensions, giving the D2V37 LBE, shown in Fig. 7(d) and its equilibrium distribution can be written as

$$f_i^{\mathrm{eq},4} = f_i^{\mathrm{eq},3} + \rho w_i \left[\frac{a^4u^4}{8} + a^2\Theta u^2 + \Theta^2 - \frac{a^6u^2}{4}(\boldsymbol{c}_i\cdot\boldsymbol{u})^2 - \frac{3a^4}{2}\Theta(\boldsymbol{c}_i\cdot\boldsymbol{u})^2 - a^2\Theta^2 c_i^2 - \frac{a^4}{4}\Theta u^2 c_i^2 + \frac{a^8}{24}(\boldsymbol{c}_i\cdot\boldsymbol{u})^4 + \frac{a^6}{4}\Theta(\boldsymbol{c}_i\cdot\boldsymbol{u})^2 c_i^2 + \frac{a^4}{8}\Theta^2 c_i^4 \right] \quad \text{(A3)}$$

with the weights and scaling factor given in Table III.

TABLE III. Weights and scaling factor of the D2V37 model.

i	w_i
0	$\frac{56266R^2-7^{2/3}(19991-338\sqrt{30})R+7^{4/3}(14323+6238\sqrt{30})}{264600R^2}$
1–4	$\frac{31206R^2-7^{2/3}(3201+466\sqrt{30})R-7^{4/3}(2427-706\sqrt{30})}{264600R^2}$
5–8	$\frac{29232R^2+7^{2/3}(3888+265\sqrt{30})R+7^{4/3}(216-1027\sqrt{30})}{529200R^2}$
9–12	$\frac{42R^2+7^{2/3}(33+2\sqrt{30})R-\sqrt[3]{7}(3+62\sqrt{30})}{3600R^2}$
13–20	$\frac{1638R^2+7^{2/3}(1647+4\sqrt{30})R-7^{4/3}(891+496\sqrt{30})}{264600R^2}$
21–24	$\frac{-126R^2+7^{2/3}(1161+194\sqrt{30})R+7^{4/3}(1107-242\sqrt{30})}{1058400R^2}$
25–28	$\frac{14R^2+7^{2/3}(131+10\sqrt{30})R+7^{4/3}(17-34\sqrt{30})}{264600R^2}$
29–36	$\frac{-168R^2+7^{2/3}(228+71\sqrt{30})R+7^{4/3}(516-29\sqrt{30})}{1058400R^2}$
a	$\frac{1}{6}\sqrt{49-\frac{17(7)^{2/3}}{R}+7^{1/3}R}$
R	$(67+36\sqrt{30})^{1/3}$

[1] G. R. McNamara and G. Zanetti, Phys. Rev. Lett. **61**, 2332 (1988).
[2] U. Frisch, B. Hasslacher, and Y. Pomeau, Phys. Rev. Lett. **56**, 1505 (1986).
[3] F. Higuera and J. Jiménez, Europhys. Lett. **9**, 663 (1989).
[4] S. Chen, H. Chen, D. Martinez, and W. Matthaeus, Phys. Rev. Lett. **67**, 3776 (1991).
[5] Y. H. Qian, D. d'Humières, and P. Lallemand, Europhys. Lett. **17**, 479 (1992).
[6] P. L. Bhatnagar, E. P. Gross, and M. Krook, Phys. Rev. **94**, 511 (1954).
[7] F. J. Alexander, S. Chen, and J. D. Sterling, Phys. Rev. E **47**, R2249 (1993).
[8] G. McNamara and B. Alder, Physica A **194**, 218 (1993).
[9] Y. Chen, H. Ohashi, and M. Akiyama, Phys. Rev. E **50**, 2776 (1994).
[10] X. He and L.-S. Luo, Phys. Rev. E **56**, 6811 (1997).
[11] P. C. Philippi, L. A. Hegele Jr., L. O. E. dos Santos, and R. Surmas, Phys. Rev. E **73**, 056702 (2006).
[12] X. Shan, X.-F. Yuan, and H. Chen, J. Fluid Mech. **550**, 413 (2006).
[13] D. N. Siebert, L. A. Hegele, Jr., R. Surmas, L. O. E. dos Santos, and P. C. Philippi, Int. J. Mod. Phys. C **18**, 546 (2007).
[14] S. Succi, *The Lattice Boltzmann Equation*, 1st ed. (Oxford University Press, New York, 2001), Chap. 14, pp. 246–247.
[15] D. d'Humières, Prog. Astronaut. Aeronaut. **159**, 450 (1992).
[16] P. C. Philippi, L. A. Hegele Jr., R. Surmas, D. N. Siebert, and L. O. E. dos Santos, Int. J. Mod. Phys. C **18**, 556 (2007).
[17] X. Shan and X. He, Phys. Rev. Lett. **80**, 65 (1998).
[18] P. Lallemand and L.-S. Luo, Phys. Rev. E **61**, 6546 (2000).
[19] J. D. Sterling and S. Chen, J. Comput. Phys. **123**, 196 (1996).
[20] P. Lallemand and L.-S. Luo, Phys. Rev. E **68**, 036706 (2003).